Nonideal plasmas as non-equilibrium media

2003 J. Phys. A: Math. Gen. 36 8723

(http://iopscience.iop.org/0305-4470/36/32/311)

INSTITUTE OF PHYSICS PUBLISHING JOURNAL OF PHYSICS A: MATHEMATICAL AND GENERAL

J. Phys. A: Math. Gen. **36** (2003) 8723–8732 PII: S0305-4470(03)60384-7

Nonideal plasmas as non-equilibrium media

I V Morozov[1], G E Norman[1,2], A A Valuev[1,2] and I A Valuev[1,2]

[1] Institute for High Energy Densities of Russian Academy of Sciences, IVTAN, Izhorskaya, 13/19, Moscow 125412, Russia
[2] Moscow Institute of Physics and Technology, Institutskii Per., 9, Dolgoprudniy, Moscow Region 141700, Russia

E-mail: bogous@orc.ru

Received 4 March 2003, in final form 19 June 2003
Published 29 July 2003
Online at stacks.iop.org/JPhysA/36/8723

Abstract

Various aspects of the collective behaviour of non-equilibrium nonideal plasmas are studied. The relaxation of kinetic energy to the equilibrium state is simulated by the molecular dynamics (MD) method for two-component non-degenerate strongly non-equilibrium plasmas. The initial non-exponential stage, its duration and the subsequent exponential stage of the relaxation process are studied for a wide range of ion charge, nonideality parameter and ion mass. A simulation model of the nonideal plasma excited by an electron beam is proposed. An approach is developed to calculate the dynamic structure factor in non-stationary conditions. Instability increment is obtained from MD simulations.

PACS numbers: 52.25.Dg, 52.25.Fi, 52.27.Gr, 52.35.Tc

1. Introduction

There has been increasing interest in non-equilibrium nonideal plasmas both in experiment [1–3] and theory [4, 5].

The conclusion [4] about the non-equilibrium state of experimental nonideal plasmas was based on the analysis of diverse experimental data, in particular on conductivity. The authors of recent experimental works [6–8] claim to have conditions close to equilibrium, but the Landau–Spitzer theory completely fails to describe the results. Nevertheless, the data can be explained by an equilibrium, but much more sophisticated theories [9–11]. The failure of the Landau–Spitzer-like theories does not imply, by themselves, that the plasma is in a non-equilibrium state. The main argument for non-equilibrium [4] was the scatter of the experimental data for the Coulomb part of plasma properties. The results for different materials, densities, and temperatures were considered and Coulomb conductivity was picked out. The latter can be presented in a reduced form as a dependence of dimensionless Coulomb conductivity on a nonideality parameter. These conductivity data assembled in this form

were published in [12] and used later in [13]. No sophisticated equilibrium theory is able to account for the scatter of reliable experimental data presented in the normalized form. A new challenge is the scatter of the EOS data of the Livermore and Sandia groups [14, 15] which is also attributed to the non-equilibrium two-temperature state [16].

There have been numerous attempts to modify the Boltzmann equation and extend it to dense systems [5, 17, 18]. In fact all these approaches are rather formal and explicit results can be obtained only for weakly nonideal systems or close to equilibrium. The authors [19] extrapolate their variant of the kinetic equation only to nonideality parameters less than unity and checked the extrapolation by the comparison with MD simulation. The authors [1–3] tried to compare their experimental results with theories for strongly non-equilibrium nonideal plasmas with multiply charged ions. They consider only simple modifications of the Landau theory [20], the binary collision approximation extended to strong scattering [21], and the density functional approach [16, 22]. Following the Landau approach [23] plasmas with singly and multiply charged ions were treated in the same way.

On the other hand, many experiments were conducted under quasi-stationary conditions. Some of experimental data on nonideal plasma properties (e.g. [24, 25]) can be explained in terms of plasma non-equilibrium [4, 26]. The most drastic effect was observed in [24] where Cs wire explosion in dense Ar atmosphere was investigated. The experimental values of electrical conductivity were three times lower than the data of other experimentalists and theoretical estimates. The conductivity data of [24] can be described [27] by the formula

$$\sigma = \omega_p/4\pi \tag{1}$$

corresponding to a highly turbulent (non-equilibrium) plasma [28, 29] with an effective collision frequency equal to the plasma frequency ω_p. An attempt to give a theoretical explanation of the mechanisms of plasma instability development was undertaken in [26]. It was shown that the beam instability could be the reason for plasma turbulence. The run-away electron beam arises at the boundaries of transverse bright and dark layers (strata) observed in the experiment. These electron beams are formed by very strong electric fields existing between the layers. The mechanisms and dynamics of strata formation were investigated in [26] as well. Some ideas concerning nonideal plasma instabilities are presented in [30].

In the present work the MD method is used to study strongly non-equilibrium nonideal plasmas. In this case the MD method is more efficient than a numerical solution of kinetic equations. The relaxation of the electron and ion kinetic energies in plasmas with multiply charged ions is considered. A beam–plasma system is simulated to investigate instability development and stationary non-equilibrium plasma states.

2. Relaxation in plasmas

We consider an electroneutral two-component system of ZN electrons and N ions with masses m and M, respectively, Z is the charge of the ion. The nonideality is characterized by the parameter $\Gamma_e = e^2(4\pi n_e/3)^{1/3}/(k_BT)$ for electrons and $\Gamma_i = Z^2e^2(4\pi n_i/3)^{1/3}/(k_BT)$ for ions, where $n_e = Zn_i$ and n_i are the electron and ion number densities, T is the temperature. The relaxation in the system of free charges is studied. A quasiclassical effective pair electron–ion potential is used so that the low energy bound states in the Coulomb well are not to be taken into account[3]. The form of the interaction potential ('corrected Kelbg') is

$$V_{cd}(r) = \frac{e_ce_d}{r}\left[F(r/\lambda_{cd}) - r\frac{k_BT}{e_ce_d}\tilde{A}_{cd}(\xi_{cd})\exp(-(r/\lambda_{cd})^2)\right]$$

[3] It should be noted that a deeper Coulomb potential (with respect to temperature) is used in studies of the recombination relaxation in ultracold plasmas [31, 32].

$$\lambda_{cd} = \hbar\Big/\sqrt{2m_{cd}k_BT} \qquad m_{cd}^{-1} = m_c^{-1} + m_d^{-1} \qquad \xi_{cd} = -(e_ce_d)/(k_BT\lambda_{cd})$$
$$F(x) = 1 - \exp(-x^2) + \sqrt{\pi}x(1 - \operatorname{erf}(x)). \tag{2}$$

The coefficients $A_{cd}(T)$ provide the exact value of the Slater sum and its first derivative at $r = 0$. The definition of these parameters can be found in [33], and other details of the simulation model in [34].

The number of ions is $N = 64$–100 in our simulation. It was shown [35–37] that, due to the screening effects in two-component plasmas with $\Gamma_e \sim 1$, each particle effectively interacts only with its nearest neighbours, and the exponential Debye law for the effective interparticle interaction remains valid for distances larger than the average interparticle distance even for $\Gamma_e > 1$. It was found that $N = 50$ was sufficient for such plasmas when calculating thermodynamic properties and correlation functions [35–37]. In this paper we performed test simulations of the relaxation in strongly non-equilibrium plasmas for N varied from 25 to 800 and found that starting from $N = 50$, the scatter of the relaxation curves for different N is within the numerical error.

Two different initial conditions are investigated for spatial configuration of ions. The first one is a crystal structure with cubic lattice which corresponds to the relaxation in solids [1, 2]. The second is a quasi-random configuration obtained from the equilibrium isothermal electron–ion plasma with the same number density. Statistically independent equilibrium configurations of electrons supplement the ensemble of initial states. In both cases the initial ion velocities are dropped to zero and the electron temperature is equal to 30 000 K. This model describes the plasma just after ionization where $T_e \gg T_i$. The results of MD simulation runs are averaged over an ensemble of $I = 48$–192 initial states in both cases. Provided the result is N-independent, the relative error is given by $1/\sqrt{NI}$. The error bars in figures correspond to the confidence coefficient of 0.68. The bars are not indicated if they are smaller than the size of the points.

The relaxation from the initial conditions given above is characterized by a decay of the difference between electron and ion kinetic energies $\Delta T = T_e - T_i$. The values of T_e and T_i are obtained as the average kinetic energy of the particles in MD simulations, $T(t) = \frac{1}{2NI}\sum_{j,k}^{N,I} mv_{jk}^2(t)$. The dependences of ΔT on time are shown in figures 1(a) and (b) for different initial conditions, the time here and below is measured in periods of electron plasma oscillations $\tau_e = 2\pi/\omega_p$. The MD simulation results are compared with the Landau theory [23] which leads to

$$\frac{\mathrm{d}T_e}{\mathrm{d}t} = -\frac{T_e - T_i}{\tau_{ei}} \qquad \tau_{ei} = \left(\frac{T_e}{T_e(0)}\right)^{3/2} \frac{M/m}{8\sqrt{3\pi}ZL_e}\Gamma_e^{-3/2}. \tag{3}$$

The solutions of this equation are presented in figure 1(c) which are the extrapolations of the Landau theory far beyond the limits of its applicability. The Coulomb logarithm L_e is set to be equal to 3. All figures 1(a)–(c) show the exponential decay $\Delta T \sim \mathrm{e}^{-t/\tau_B}$ in the relaxation tail. The duration of the initial non-exponential stage is denoted as τ_{nB}. Both times τ_B and τ_{nB} are shown in figure 1(d) depending on Z for MD results. The deviations from the Landau theory (3) are as follows. First, the exponent τ_B is greater for MD simulations by more than two orders of magnitude in accordance with [1, 2]. Second, MD simulation shows that the duration of the initial non-exponential stage τ_{nB} is greater than the theoretical one in the case of crystal-like initial conditions. As seen from figure 1(d) it grows exponentially with Z while τ_B remains almost constant. Thus for $Z > 3$ the non-exponential stage becomes the predominant stage of the relaxation. It should be noted that while the non-exponential stage is strongly dependent on the initial conditions the time τ_B is almost independent of it. This agrees with the earlier results [38].

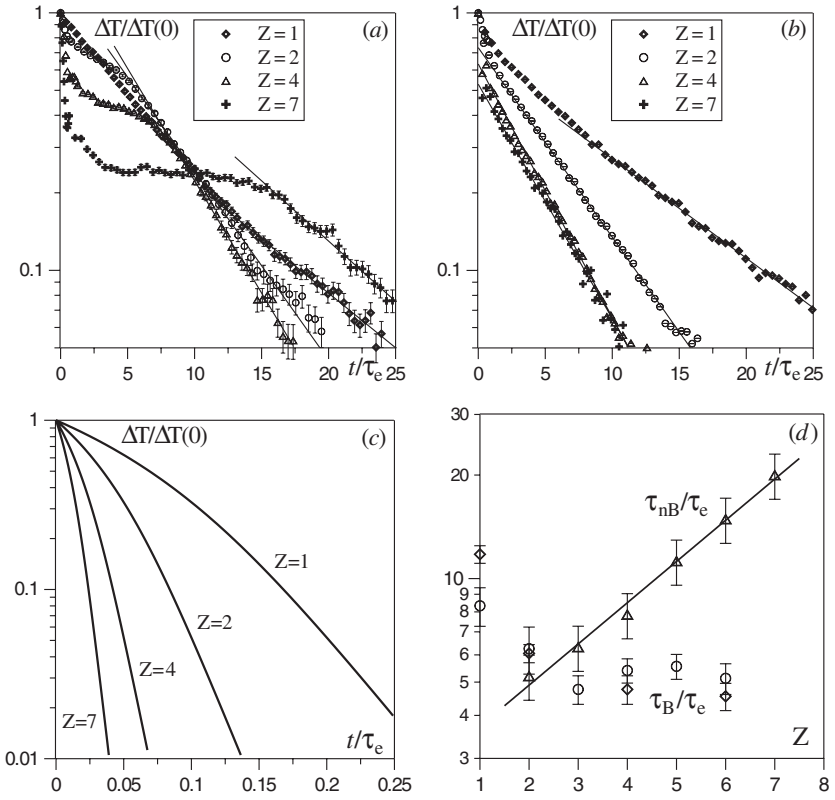

Figure 1. (*a*)–(*c*) The difference between the average kinetic energies of electrons and ions $\Delta T = |T_e - T_i|$ depending on time for different ion charges Z: MD simulations for crystal-like (*a*) and quasi-random (*b*) initial conditions, ideal plasma theory [23] (*c*). (*d*) The dependence of the relaxation times on the ion charge Z for crystal-like initial conditions: circles—τ_B, triangles—τ_{nB} and quasi-random initial conditions: rhombus—τ_B. $M/m = 100$, $\Gamma_e = 1.28$.

Table 1. The dependence of the exponents α_B and α_{nB} (4) on Z for $\Gamma_e = 1.28$.

Z	α_B	α_{nB}
1	0.85 ± 0.01	–
2	0.90 ± 0.03	0.94 ± 0.01
4	0.84 ± 0.04	0.99 ± 0.02
7	0.67 ± 0.09	1.00 ± 0.02

Figures 2(*a*)–(*c*) show the dependence of the relaxation times on the ion–electron mass ratio M/m for crystal-like initial conditions. It is seen that for each value of Z, it is possible to draw power fits

$$\tau_B \sim (M/m)^{\alpha_B} \qquad \tau_{nB} \sim (M/m)^{\alpha_{nB}}. \tag{4}$$

The coefficient α_B depends on Γ as shown in figure 2(*d*). It tends to 1 in the ideal plasma limit ($\Gamma_e \to 0$) in accordance with (3). The dependences of both α_B and α_{nB} on Z are given in table 1.

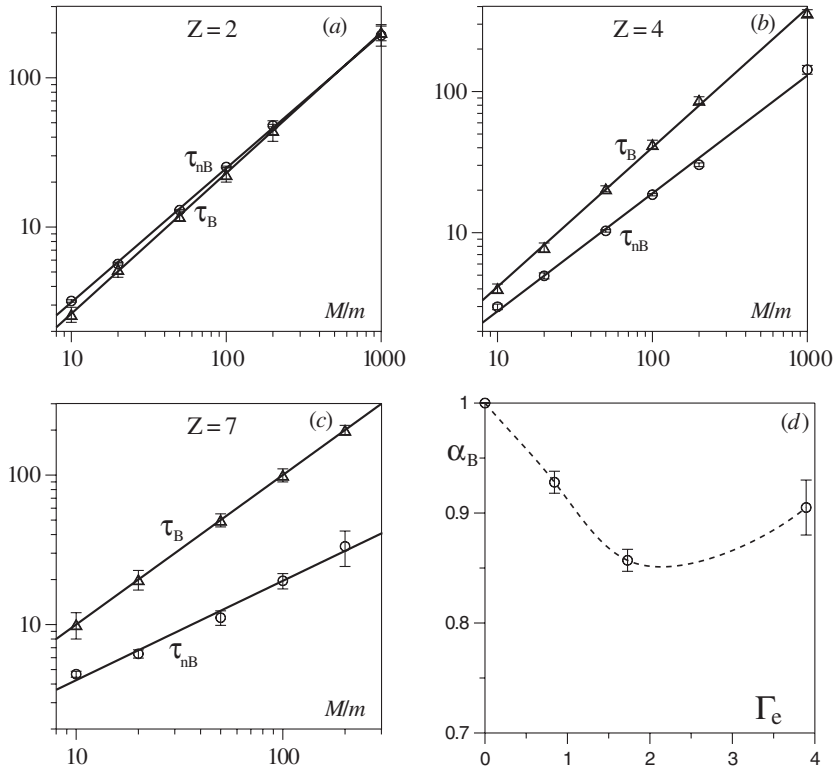

Figure 2. (*a*)–(*c*) The dependence of the relaxation times τ_B (circles) and τ_{nB} (triangles) on the electron–ion mass ratio for different ion charges *Z*. All mass dependences are fitted by power fits. $\Gamma_e = 1.28$. (*d*) The dependence of the coefficient α_B (4) on Γ_e for $Z = 1$.

Using the given Γ-dependence and mass dependence one can estimate the relaxation times in real experimental conditions. In the case of experiments with shock compressed aluminium [2] ($T_e(0) = 2.4\,\mathrm{eV}$, $n_e = 1.2\,\mathrm{g\,cm^{-3}}$, $\Gamma_e = 4.1$, $Z = 3$) we obtain the relaxation times $\tau_B = 0.4$ ps, $\tau_{nB} = 4$ ps. The error in determining coefficients α_B and α_{nB} is about $\xi_\alpha = 5\%$. The corresponding error of extrapolation of relaxation times is $\xi_\tau = \log(M_r/M)\xi_\alpha = 40\%$, where M_r/M is the ratio between real and model ion masses. The obtained precision is enough for comparison by an order of magnitude.

3. Stationary non-equilibrium

The non-equilibrium appears due to the initial conditions of the plasmas considered in the previous section. The plasma then relaxes to its equilibrium state with all its parameters approaching equilibrium ones in the course of time evolution. In this section we consider a stationary non-equilibrium caused by an electron beam propagating with a constant velocity through the plasma. This type of non-equilibrium exists in some experiments when large electron flows arise in plasma. The aim of this simulation was to detect the excitation of non-equilibrium collective plasma oscillations which are permanently present in the case of beam-excited plasma.

A model of hydrogen plasma (with realistic electron to ion mass ratio) consisting of 200 to 600 particles placed in the box with periodic boundary conditions is used in MD simulation. The choice of the number of particles does not influence very much the results of all simulations presented below, except for the better smoothness of the dynamic structure factors for larger systems. The number of particles chosen is sufficient to study oscillations at plasma frequencies [39]. We use a cut-off pseudopotential, where the electron–ion Coulomb pair interaction is replaced by a constant ($3kT$) at cohesive energies greater than $3kT$, in this part of the work. Electron–electron and ion–ion interactions are described by electrostatic repulsion [39]. The equilibrium state prepared by the Monte Carlo procedure is used as the initial condition for the MD experiment. The initial equilibrium parameters are $\Gamma = 1, T = 30\,000$ K for the plasma.

Then a number of extra electrons, which simulate the beam, are driven through the system in one direction with constant velocity vector. The entry point is randomly selected for each extra electron entering the simulation cell and reselected when it crosses the cell boundary. The extra electrons interact with plasma particles, but their own velocities and trajectories are kept unchanged, once selected. Typical parameters of the beam are: density $n_b = \alpha n_e$, velocity $V = 3v_T$, where $\alpha = 0.03$, n_e is the plasma electron density and $v_T = \sqrt{3k_BT/m_e}$ is the electron thermal velocity in equilibrium.

The time evolution of the component energies of the system is shown in figure 3(a). Electrons are heated up faster than ions, therefore a two-temperature plasma arises as the result of beam excitation.

The superthermal excitation of plasma oscillations can be detected by comparing the dynamic structure factors (DSFs) of the plasma under consideration [39–41] for different **k**-vectors with those characterizing the equilibrium case. The oscillations show up as enhanced and shifted peaks of the DSF and corresponding changes in the dispersion curve $\omega_{\max}(k)$.

The temperature of electrons grows too rapidly due to beam excitation for direct measurement of DSF in the MD experiment, which requires averaging over a relatively long period of time without significant change of the system characteristics. To overcome this difficulty, the same idea is applied to withdraw the energy from the system and keep the average electron temperature constant for the period of DSF measurement. The beam-excited system is simulated until the electron temperature reaches some value T_m at time t_m. Then the simulation of the system is continued with additionally applied velocity scaling at every time step which retains the electron temperature at the constant level T_m. This is performed for the period which is sufficient to measure DSF. The resulting DSF characterizes the level of plasma excitation by the beam at the time moment t_m. The close idea of freezing non-equilibrium state was applied in [42].

An example of DSFs measured at temperatures $T_{m1} = 1.2T_0 = 36\,000$ K and $T_{m2} = 1.8T_0 = 54\,000$ K is shown in figures 3(b)–(d) for different k-values compared with the equilibrium DSF. The corresponding points in the time evolution are marked by open circles in figure 3(a). As expected, the DSFs show a remarkable change of intensity in the peak regions in the case of beam excitation.

In order to be sure that the properties of the system with a beam do not change while the velocities are being scaled we check the pair correlation functions (figure 4(a)) and electron velocity distribution function (figure 4(b)) averaged over two consequent subintervals of the DSF measurement period. The duration of these subintervals is $1500/\omega_p$. Beam particles are not taken into account when calculating velocity and pair distributions. As is seen from the figures, the pair correlation function remains the same for the whole measurement interval. The velocity distributions for two subintervals are also very close to each other and to the Maxwellian one. This allows us to assume that velocity scaling does not change

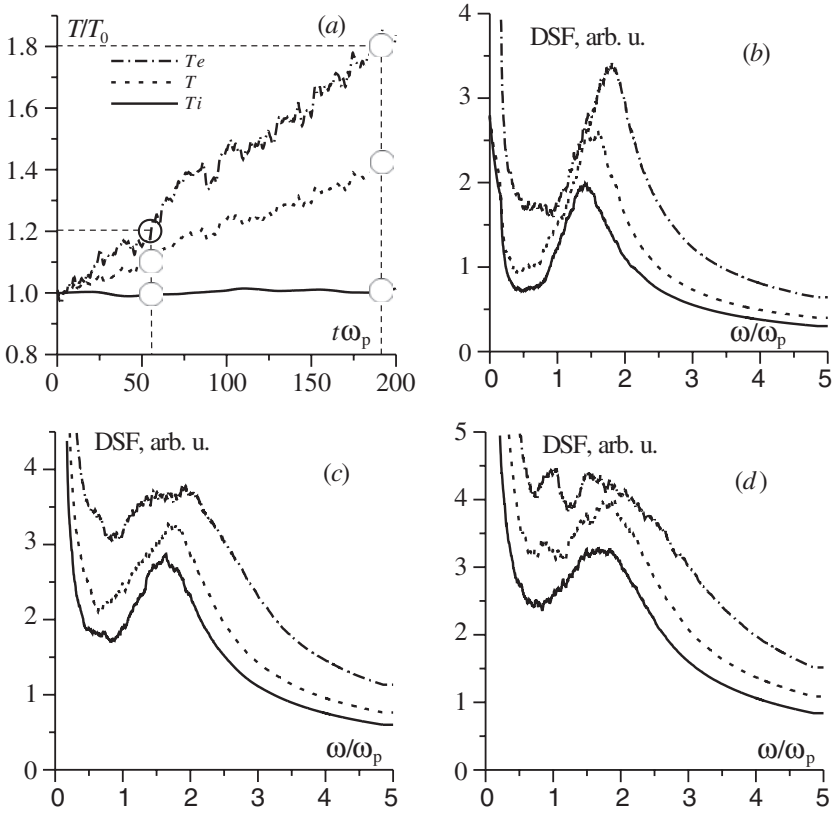

Figure 3. (*a*) Time evolution of the component temperatures during beam excitation. The points of DSF measurement are marked by open circles. (*b*)–(*d*) Dynamic structure factors for different stages of plasma excitation drawn for the first three minimum **k**-vectors allowed in the MD cell of the size selected in the simulation. Solid curves represent the equilibrium DSF, dashed lines DSF at $t = 56/\omega_p$ and dot-dashed lines DSF at $t = 182/\omega_p$. (*b*) $\mathbf{k} = 0.34R_D^{-1} = 1.49 \times 10^9\ \mathrm{m}^{-1}$; (*c*) $\mathbf{k} = 0.49R_D^{-1} = 2.15 \times 10^9\ \mathrm{m}^{-1}$; (*d*) $\mathbf{k} = 0.59R_D^{-1} = 2.59 \times 10^9\ \mathrm{m}^{-1}$, where R_D is the Debye length in equilibrium. The same arbitrary units are used for (*b*)–(*d*).

the microscopic properties of the system significantly and serves only as a mechanism of additional cooling.

The time dependence of the ratio of maximum value of non-equilibrium DSF to the equilibrium one $S_m(t)/S_m(0)$ is presented in figure 5(*a*) for three values of k. The greater k does not manifest any instability development. The exponential fit of the data gives the exponent of the squared growth of the collective electric field. Half of the exponent is the instability increment, figure 5(*b*).

According to the theory for weakly collisional plasma the hydrodynamic and kinetic instabilities can be developed for the selected plasma parameters. In fact (see e.g. [43]), two instability conditions must be satisfied for a collisional plasma:

$$\tau\delta \gg 1 \tag{5}$$

$$\delta = \delta_{cl} - \nu > 0 \tag{6}$$

where τ is the relaxation time of a perturbation, δ is an instability increment (that is $\delta = \mathrm{Im}\,\omega$, ω is a solution of the dispersion equation), δ_{cl} is the increment for collisionless plasma and

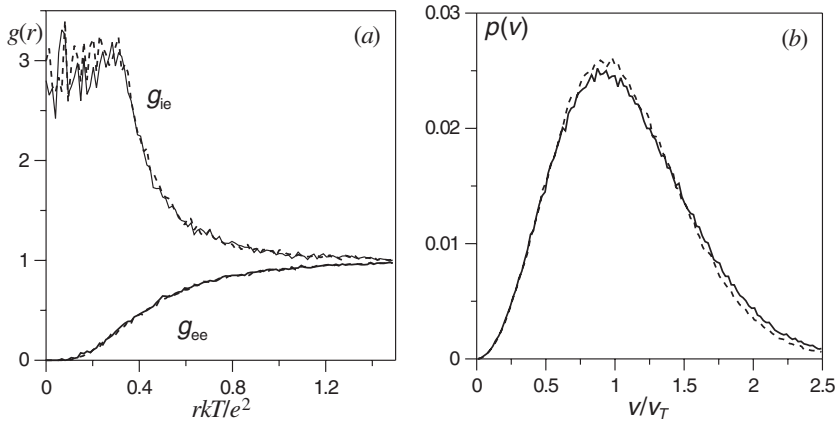

Figure 4. Microscopic distributions of the beam-excited system under velocity scaling for two subintervals of the DSF measurement period. The first half of the whole interval of duration $3000/\omega_p$ is represented by solid lines, and the second half by dashed lines. (*a*) Pair correlation function for electron–electron (g_{ee}) and ion–electron (g_{ie}) correlations. (*b*) Electron velocity distribution function. $v_T = \sqrt{3k_BT/m_e}$ is the electron thermal velocity.

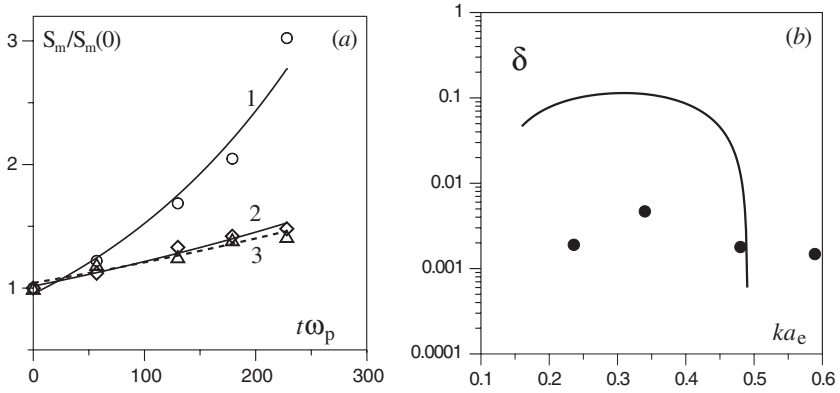

Figure 5. (*a*) Time dependence of DSF maximum to the equilibrium DSF maximum ratio: circles—$ka_e = 0.34$, rhombus—$ka_e = 0.48$, triangles—$ka_e = 0.59$; curves 1–3—corresponding exponential fits. (*b*) *k*-dependence of instability increment: points—MD simulation, dashed line—schematic drawing of hydrodynamic instability increment [43].

ν is the collisional damping decrement of plasma waves. For the parameters selected in the MD experiment the maxima of both hydrodynamic and kinetic instability increments have the same order of magnitude and are reached at $ka_e \approx v_{Te}/V$ and $\omega \approx \omega_p$. The value of the δ_{cl} can be estimated by the following equation:

$$\delta_{cl}/\omega_p = 3^{1/2}2^{-4/3}\alpha^{1/3} \approx 0.2. \tag{7}$$

According to [44] the collision damping decrement ν/ω_p at $\Gamma \approx 1$ cannot be greater than 0.1. Thus, $\delta/\omega_p \approx 0.1 > 0$ and (6) is satisfied.

The estimation of the beam relaxation time is given by [43]

$$\tau \approx \alpha^{1/3}\,(V/v_{Te})^{3/2}\,\tau_e \tag{8}$$

where τ_e is the Maxwellization time of plasma electrons. The latter for nonideal plasma can be evaluated using the MD results of [38] $\tau\omega_p \approx 0.1\pi$. Substituting the corresponding values in (5) one obtains $\tau\delta \approx 15 \gg 1$.

Thus, both beam instability conditions (5) and (6) are satisfied. We compare our simulation results on instability increment with the predictions of [43] in figure 5(*b*). It is seen that the results of the MD simulation qualitatively agree with this theory concerning the decrement maximum position and the values of k at which the instability ceases to develop. The quantitative discrepancy is not surprising. It may result from, e.g., rude estimation of collisional damping, from the fact that the MD simulation is performed on the nonlinear stage of instability and poor applicability of the ideal plasma theory to the nonideal plasma at all.

4. Conclusion

The collective behaviour of nonideal plasma is studied for different ion charges Z.

The time dependence of the relaxation of the kinetic energy changes drastically for large Z. The duration of the non-exponential relaxation stage increases exponentially with Z for crystal-like initial conditions and becomes predominant for $Z > 3$. The dependence of the exponential stage of the relaxation of the initial conditions was not observed.

The collective behaviour of nonideal plasma results in the excitation of diverse instabilities. The extrapolation of the ideal plasma macroscopic instability theory to the nonideal plasma shows that, at least, beam instability can be developed in nonideal plasma. MD simulation confirms the fact that the instability does take place.

The comparison of MD simulation results with the extrapolated theory shows qualitative (but not quantitative) agreement. It means that the maximum instability increment lies at k-values predicted by the theory [43]. The instability does not manifest at higher values of k in accordance with the hydrodynamics instability theory as well.

Acknowledgments

The authors are grateful to V G Morozov for useful comments. This research is partially supported by the programme 'Thermophysics and Mechanics of the Intensive Energy Impacts' of Russian Academy of Science, 'Integratsiya' projects U0022 and I0661, by grants 03-07-90272v and 03-07-06102mas (IAV) of Russian Foundation of Basic Research. The computations were performed in the computer cluster system granted by Deutscher Akademischer Austauschdienst. We thank the referees, whose comments helped us to revise and improve the manuscript.

References

[1] Ng A, Celliers P, Hu G and Forsman A 1995 *Phys. Rev.* E **52** 4299
[2] Riley D, Woolsey N C, McSherry D, Weaver I, Djaoui A and Nardi E 2000 *Phys. Rev. Lett.* **84** 1704
[3] Wysocki F, Benage J, Delamater D, Montgomery D S, Murillo M S, Roberts J P and Taylor A J 2002 *SCCS 02*
[4] Norman G E and Valuev A A 1998 *Strongly Coupled Coulomb Systems*ed G Kalman, M Rommel and K Blagoev (New York: Plenum) p 103
[5] Bonitz M (ed) 2000 *Progress in Nonequilibrium Green's Functions* (Singapore: World Scientific)
[6] DaSilva A W and Katsouros J D 1998 *Phys. Rev.* E **57** 5945
[7] Benage J F, Shanahan W R and Murillo M S 1999 *Phys. Rev. Lett.* **83** 2953
[8] Haun J, Kunze H-J, Kosse S, Schlanges M and Redmer R 2002 *Phys. Rev.* E **65** 046407
[9] Kulbrodt S and Redmer R 2000 *Phys. Rev.* E **62** 7191
[10] Perrot F and Dharma-wardana M W C 1999 *J. Thermophys.* **20** 1299

[11] Desjarlais M P, Kress J D and Collins L A 2002 *Phys. Rev.* E **66** 025401(R)
[12] Norman G E and Valuev A A 1979 *Plasma Phys.* **21** 531
[13] Kraeft W D, Kremp D, Ebeling W and Röpke R 1986 *Quantum Statistic of Charged Particle Systems* (Berlin: Akademie)
[14] Collins L A, Bickham S R, Kress J D, Mazevet S, Lenosky T J, Troullier N J and Windl W 2001 *Phys. Rev.* B **63** 184110
[15] Knudson M D, Hanson D L, Bailey J E, Hall C A, Asay J R and Anderson W W 2001 *Phys. Rev. Lett.* **87** 225501
[16] Dharma-wardana M W C and Perrot F 2001 *Phys. Rev.* E **63** 069901
[17] Klimontovich Yu L 1995 *Statistical Theory of Open Systems* (Dordrecht: Kluwer)
[18] Zubarev D N, Morozov V G and Röpke G 1996 *Statistical Mechanics of Nonequilibrium Processes* (Berlin: Akademie)
[19] Bornath Th, Schlanges M, Hilse P and Kremp D 2001 *Phys. Rev.* E **64** 026414
[20] Hazak G, Zinamon Z, Rozenfeld Y and Dharma-wardana M W C 2001 *Phys. Rev.* E **64** 066411
[21] Gericke D O, Murillo M S and Schlanges M 2002 *Phys. Rev.* E **65** 036418
[22] Dharma-wardana M W C 2001 *Phys. Rev.* E **64** 035401
[23] Lifshitz M E and Pitaevskii L P 1979 *Physical Kinetics* (Moscow: Nauka) (in Russian)
[24] Dikhter I Ya and Zeigarnik V A 1976 *Dokl. Akad. Nauk* **227** 656 (in Russian)
[25] Mintsev V B and Zaporoghets Yu B 1989 *Contrib. Plasma Phys.* **29** 493
[26] Batenin V M, Berkovskii M A, Valuev A A and Kurilenkov Yu K 1987 *High Temp.* **25** 145, 299
[27] Kurilenkov Yu K and Valuev A A 1984 *Beitr. Plasmaphys.* **24** 529
[28] Artzimovich L A and Sagdeev P Z 1979 *Fizika Plasmy dlya Fizikov* (Moscow: Atomizdat) (in Russian)
[29] Alexandrov A F, Bogdankevich L S and Rukhadze A A 1984 *Principles of Plasma Electrodynamics* (Heidelberg: Springer)
[30] Kalman G J and Rosenberg M 2003 *J. Phys. A: Math. Gen.* **36** 5963
[31] Kuzmin S G and O'Neil T M 2002 *Phys. Rev. Lett.* **88** 065003
[32] Kuzmin S G and O'Neil T M 2002 *Phys. Plasmas* **9** 3743
[33] Ebeling W, Norman G E, Valuev A A and Valuev I A 1999 *Contrib. Plasma Phys.* **39** 61
[34] Morozov I V, Norman G E and Valuev A A 2001 *Phys. Rev.* A **63** 036405
[35] Zelener B V, Norman G E and Filinov V S 1974 *High Temp.* **12** 235
[36] Valuev A A, Norman G E and Filinov V S 1974 *High Temp.* **12** 818
[37] Zamalin V M, Norman G E and Filinov V S 1977 *Monte Carlo Method in Statistical Thermodynamics* (Moscow: Nauka) (in Russian)
[38] Morozov I V and Norman G E 2003 *J. Phys. A: Math. Gen.* **36** 6005
[39] Morozov I V, Norman G R and Valuev A A 1998 *Dokl. Phys.* **43** 609
[40] Hansen J P and McDonald I R 1981 *Phys. Rev.* A **23** 2041
[41] Norman G E, Valuev A A and Valuev I A 2000 *J. Physique* **10** 255
[42] Gibbon P and Pfalzner S 1998 *Phys. Rev.* E **57** 4698
[43] Mikhailovskiy A B 1970 *Teoria Plasmennyh Neustoichivostey* (Moscow: Atomizdat) (in Russian)
[44] Valuev A A, Kaklyugin A S and Norman G E 1998 *JETP* **86** 480